Scripta Materialia 186 (2020) 84–88

Contents lists available at ScienceDirect

Scripta Materialia

journal homepage: www.elsevier.com/locate/scriptamat

# Large enhancement of magnetocaloric effect driven by hydrostatic pressure in HoCuSi compound

Jia-Zheng Hao[a,b], Feng-Xia Hu[b,c,d,*], Hou-Bo Zhou[b,c], Wen-Hui Liang[b,c], Zi-Bing Yu[b,c], Fei-Ran Shen[b,c], Yi-Hong Gao[b,c], Kai-Ming Qiao[b,c], Jia Li[b,c], Cheng Zhang[b,c], Bing-Jie Wang[a,b], Jing Wang[b,c,e,*], Jun He[a,*], Ji-Rong Sun[b,c,d], Bao-Gen Shen[b,c,d,*]

[a] Division of Functional Material Research, Central Iron and Steel Research Institute, Beijing 100081, China
[b] Beijing National Laboratory for Condensed Matter Physics & State Key Laboratory of Magnetism, Institute of Physics, Chinese Academy of Sciences, Beijing 100190, China
[c] School of Physical Sciences, University of Chinese Academy of Sciences, Beijing 100049, China
[d] Songshan Lake Materials Laboratory, Dongguan, Guangdong 523808, China
[e] Fujian Innovation Academy, Chinese Academy of Sciences, Fuzhou, Fujian 350108, China

ARTICLE INFO

*Article history:*
Received 13 March 2020
Revised 5 April 2020
Accepted 16 April 2020

*Keywords:*
Magnetocaloric effect
Phase transformation
Magnetic materials

ABSTRACT

Dual field driven caloric effect has aroused great interest in recent years. Hydrostatic pressure can shift the temperature zone of magnetocaloric effect(MCE), but seldom enhance its magnitude. Here, a large enhancement of MCE driven by pressure under magnetic field available by permanent magnet has been achieved in HoCuSi compound without introducing hysteresis loss, which is favorable for developing hybrid field driven refrigeration applications at low temperature regions. A distinct mechanism is revealed. Pressure largely regulates non-collinear spin structure and magnetizing process through affecting crystal field interactions and spin-spin coupling, hence resulting in the significant impact on magnetic properties and MCE.



Solid-state refrigeration based on magnetocaloric effect (MCE) offers environmental friendly and energy-efficient solutions to displace conventional gas compression refrigeration technology [1–6]. New strategies are required to enhance the MCE to meet the needs of advanced materials that may be used in the refrigeration technologies. In addition to exploring new materials, dual-field regulation of MCE has become a current hotspot [7–12]. Physical pressure, as a clean means of regulating atomic distance and local environments, has been successfully used to tune temperature range [7,8] and reduce hysteresis loss [11,13] through impacting the magnetostructural/magnetoelastic transition for the giant MCE materials. However, the magnitude of MCE was seldom enhanced by physical pressure [7,9,14] except for few cases [8,10] where the enhanced MCE mainly originates from the enhanced contribution of lattice and the strengthening of first-order transition by pressure. In this case, hysteresis loss is inevitably introduced, which damages the effective refrigeration capacity.

Here, we report large enhancement of MCE without introducing hysteresis loss by hydrostatic pressure in HoCuSi. A new mechanism is revealed. This compound has been previously identified as an attractive magnetic refrigerant owing to its reversible giant MCE around Néel temperature $T_N$~7 K [15]. The reported magnetic entropy change (-$\Delta S$~33.1 J kg$^{-1}$K$^{-1}$, 5T) approaches to that (-$\Delta S$~36 J kg$^{-1}$K$^{-1}$) of $ErCo_2$, the most representative magnetic refrigerant in the low temperature region [1,16,17]. As well known, low temperature refrigeration also has broad applications in various areas, [16,18] such as space science and liquefaction of natural gas/hydrogen, in addition to the familiar requirements of refrigeration around room temperature. Exploring MCE as high as possible is always a challenge and a long-term pursuit.

As a member of RCuSi family (R, heavy rare earth elements), HoCuSi compound with hexagonal $Ni_2In$-type structure shows complex spin structure and abundant magnetic phase transition. Previous neutron diffraction study [19] revealed that HoCuSi is an antiferromagnet (AFM) with Néel temperature around $T_N$~9 K. Below $T_N$, the spin structure formed by $Ho^{3+}$ ions is a sine wave modulation structure with a propagation vector $k = (1/15,0,1/6)$. The direction of $Ho^{3+}$ magnetic moment forms angle of 61(6)° with the c-axis and 132(6)° with the a-axis. Such magnetic order is stable in the temperature range between 1.4 K and $T_N$ [19]. Strain measurements [15] showed that there is a mutation in the lattice constant near the $T_N$, and the magnetic ordering with such a

* Corresponding authors.
*E-mail addresses:* fxhu@iphy.ac.cn (F.-X. Hu), wangjing@iphy.ac.cn (J. Wang), hejun@cisri.com.cn (J. He), shenbg@iphy.ac.cn (B.-G. Shen).

https://doi.org/10.1016/j.scriptamat.2020.04.019
1359-6462/

complex spin structure is closely related to the lattice mutation in HoCuSi. Crystal field effect (CFE) and the competition with magnetic interaction play dominating roles in the formation of non-collinear spin structures and lead to unusual magnetic properties [20,21]. Theoretical calculations, for a hexagonal symmetry structure, indicated that the easy axis of magnetization is parallel to the c-axis if the second-order crystal field parameter $B_2^\circ$ is negative, the case of RCuSi with $R$ = Er and Tm, while the easy axis tends to perpendicular to or form an angle with the c-axis if the $B_2^\circ$ is positive, the case of RCuSi with $R$ = Tb, Dy, Ho [22,23]. Normally, the magnitude and direction of the crystal field of the rare earth ions affect the orientation of the total angular momentum, and the crystal field is closely related to the crystal structure and atomic local environments. Therefore, physical pressure can modulate the spin structure through impacting the atomic distances and local environments of rare earth atoms, thereby ultimately regulating the magnetic properties and the MCE.

Here, we report the effect of hydrostatic pressure on the magnetic properties and MCE in HoCuSi compound. It is found that the applied pressure can enhance the both effective magnetic moment ($M_{eff}$) and paramagnetic Curie temperature ($\theta_P$), illustrating that the ferromagnetic (FM) coupling between $Ho^{3+}$ ions is favored through modulating the non-collinear spin structure by the pressure-induced compression of Ho-Ho distance and alteration of local environments. The application of pressure regulates the magnetization process. When a pressure 6.6kbar is applied, the 1T, 2T and 5T magnetization at 5 K increases by ~46%, ~28%, and ~11%, respectively, but no hysteresis loss is introduced even at the phase transition region. Based on Maxwell relation, $\Delta S$ and hence the refrigeration capacity (RC) are calculated. Increasements of 150%(0–1T) and 67%(0–2T) in the completely reversible $\Delta S$ are achieved when a pressure of 6.6 kbar is applied, and the corresponding RC increases by 134%(0–1T) and 73%(0–2T), respectively.

Polycrystalline HoCuSi was prepared by arc melting the constituent elements (Ho with purity 99.5% and Cu, Si with purity 99.99%) followed by vacuum annealing for 7 days at 1123 K, and then quenched in liquid nitrogen. The rare earth Ho was added in excess of 5% considering its volatilization. Magnetic measurements under pressure were performed using SQUID (MPMS-7T). Hydrostatic pressure was applied through a commercial Be-Cu pressure cell specially designed for SQUID, where Daphne 7373 oil acts as the pressure transmitting medium. The applied pressure was determined by measuring the superconducting transition temperature of the standard sample Pb placed with the sample in the cell.

Crystal structure was determined by powder X-ray diffractometer (XRD) using Cu-K$\alpha$ target. The Rietveld refined XRD pattern of HoCuSi compound at room temperature is given in Fig. 1. The sample crystallizes in $Ni_2In$-type hexagonal structure with space group $P6_3/mmc$ (SG #194), as shown in the inset of Fig. 1. No impurity phase was detected. The lattice parameters were refined to be $a = b = 4.14001(4)$Å, $c = 7.36848(1)$ Å, consistent with the previously reported[15, 19]. HoCuSi compound has layered structure with large distance between Ho atoms. The in-plane Ho-Ho bond length is 3.68424(5) Å while the inter-plane Ho–Ho bond length is 4.14001(4)Å. Hence, the rare earth $Ho^{3+}$ ions form a local magnetic moment through Ruderman-Kittel-Kasuya-Yosida (RKKY) type exchange interaction [19]. For HoCuSi, the Hamiltonian can be expressed as,

$$\widehat{H} = -H_{mag} + H_{cfe} - H_{Zeeman} = -\sum_{il}\lambda_0(r)J_i.J_l + \lambda_1(r)[J_i.J_l]^2 - g\mu_B\sum_i J_i H. \quad (1)$$

where the first term is the spin-spin interaction, $J_i$ represents the total angular momentum operator of Ho ions, and $\lambda_0$ is the exchange integral, which mainly depends on the distance between Ho-Ho neighbors. The second term describes crystal field

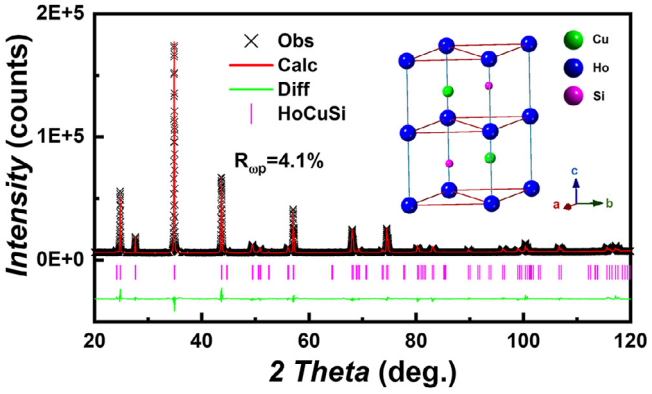


**Fig. 1.** The Rietveld refined X-ray powder diffraction pattern of HoCuSi compound at room temperature. The observed profile (black cross), calculated profile (red line), their difference (blue line), Bragg reflection positions (magenta bar), and error factor $R_{wp}$ are indicated. Inset shows the schematic diagram of the $Ni_2In$-type hexagonal structure for HoCuSi, where the intra-plane Ho-Ho bonds are denoted by red while the inter-plane Ho–Ho bonds denoted by blue. (For interpretation of the references to colour in this figure legend, the reader is referred to the web version of this article.)

interactions, where $\lambda_1$ is the parameter of the model. Changes in the crystal structure and local environments of ions will cause corresponding changes in crystal field interactions. The third term represents the Zeeman interaction, where H is the applied magnetic field, g is the Lande‘ factor and $\mu_B$ is the Bohr magneton [21,24]. Physical pressure changes the lattice parameters and the distances between Ho atoms, consequently leading to changes in magnetic exchange interactions and crystal field interactions. In other words, physical pressure is able to affect the competition between spin-spin exchange and crystal field interactions, and hence regulate the spin structure.

Fig. 2a shows the thermomagnetic(M–T) curves measured in 0.01T magnetic field under different pressures for HoCuSi. Both the zero-field-cooled (ZFC) heating and field-cooling (FC) M–T curves exhibit maxima around $T_N$, indicating a phase transition from AFM to paramagnetic (PM) state. The $T_N$ at ambient pressure is about 6.9 K, which is nearly the same as the reported in Ref.15. The ZFC and FC branches completely coincide above $T_N$. With the increase of pressure, the $T_N$ hardly changes, but the peak magnetization shows significant increase from 1.15 $Am^{-2}kg^{-1}$ at 0 kbar to 3.21 $Am^{-2}kg^{-1}$ at 9.0 kbar. A peak below the $T_N$ can be identified, which may be originated from spin orientation transition (see details in supplementary materials). In addition, the reciprocal of susceptibility $1/\chi$ obeys the Curie-Weiss law in the PM region for each pressure (inset of Fig. 2a). Accordingly, the $M_{eff}$ and the $\theta_P$ can be evaluated from the slope and the extrapolation of the linear part of $1/\chi$-T curve according to $\frac{1}{\chi} = \frac{3k_B}{NM_{eff}^2}(T-\theta_P)$, where N denotes the number of atoms per mole, $k_B$ is the Boltzmann constant [15,19]. At ambient pressure, the obtained $M_{eff}$ is about 10.07 $\mu_B/Ho^{3+}$, which is slightly lower than the moment of $Ho^{3+}$ free ions (~10.60 $\mu_B/Ho^{3+}$), while the $\theta_P$ is about 3.6 K. The positive $\theta_P$ indicates that the $Ho^{3+}$ in HoCuSi may have FM short-range interactions in the PM state [15, 19]. Physical pressure favors FM coupling between $Ho^{3+}$ ions through regulating the non-collinear sine wave modulated spin structure by the pressure-induced compression of Ho–Ho distance, and the $M_{eff}$ shows a slight increase with increasing pressure (see Fig. 2b, Table 1). When the pressure is increased to 9.0 kbar, the $M_{eff}$ approaches to the moment of $Ho^{3+}$ free ions (~10.60 $\mu_B/Ho^{3+}$). Moreover, the $\theta_P$ also moves to high temperature from 3.6 K at ambient pressure to 8.2 K at 9.0 kbar (Fig. 2b, Table 1). This result further demonstrates that the FM exchange interaction is significantly enhanced by pressure.

**Table 1**
The Néel temperatures $T_N$, paramagnetic Curie temperatures $\theta_P$, effective magnetic moments $M_{eff}$, critical magnetic field inducing metamagnetic transition $H_C$, 1T, 2T and 5T magnetization at 5 K and the correspondingly enhanced ratio under different pressures for HoCuSi compound.

| P.(kbar) | $T_N$.(K) | $\theta$p.(K) | $M_{eff}$.($\mu_B$) | Hc.(T) | M(1T).($Am^2kg^{-1}$) | Enh.M(1T) | M(2T).($Am^2kg^{-1}$) | Enh.M(2T) | M(5T).($Am^2kg^{-1}$) | Enh.M(5T) |
|---|---|---|---|---|---|---|---|---|---|---|
| 0 | 6.9 | 3.6 | 10.07 | 0.35 | 104.9 | – | 149.9 | – | 200.3 | – |
| 4.4 | 6.7 | 4.5 | 10.35 | 0.30 | 140.6 | 34.0% | 183.5 | 22.4% | 222.0 | 10.8% |
| 6.6 | 6.5 | 7.0 | 10.55 | 0.25 | 153.5 | 46.3% | 191.3 | 27.6% | 223.2 | 11.4% |
| 9.0 | 6.7 | 8.2 | 10.59 | 0.20 | 165.8 | 58.1% | 195.6 | 30.5% | 223.4 | 11.5% |

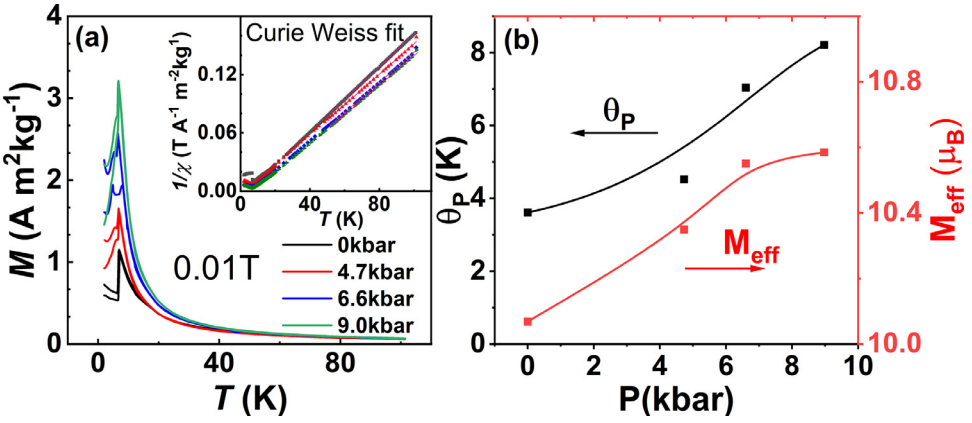


**Fig. 2.** (a) Temperature dependences of the ZFC and FC magnetizations for HoCuSi in a magnetic field of 0.01 T under different pressures. The inset shows $1/\chi$-T curves under different pressures. (b) The pressure dependences of paramagnetic Curie temperature $\theta_P$ and effective magnetic moment $M_{eff}$ derived by Curie-Weiss law based on the M–T curves.

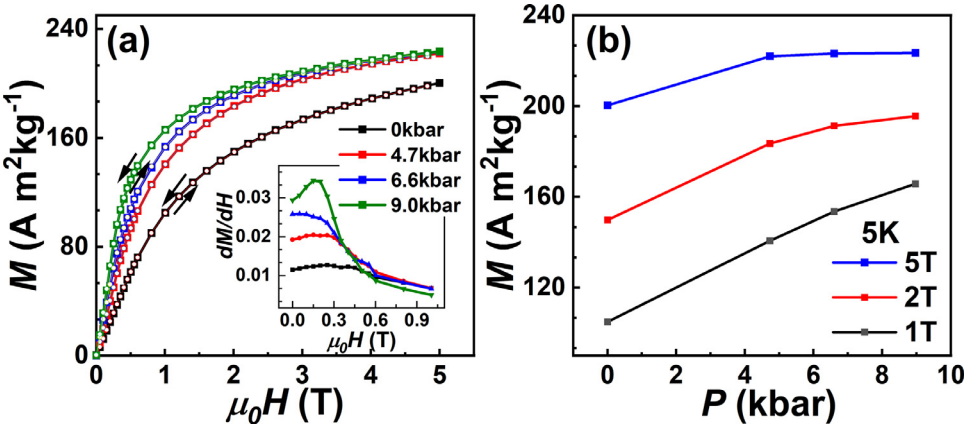


**Fig. 3.** (a) Magnetization isotherms of HoCuSi compound measured on increasing (solid squares) and decreasing field (open circles) at 5 K under different pressures, where the arrows indicate the ramping direction of magnetic field. Inset shows the corresponding dM/dH vs.T curves. (b) Pressure dependence of 1T, 2T and 5T magnetization at 5 K.

Physical pressure compresses the Ho-Ho distance and affect the local environments, leading to simultaneous changes in magnetic exchange and CFE, thereby regulating the spin structure and the magnitude of magnetic moment.

Fig. 3a presents the isothermal magnetization (M–H) curves of HoCuSi measured on increasing and decreasing field at 5 K under different pressures. No hysteresis occurs under all pressures. Here, it is noteworthy that the different magnetizing process enforced by pressure is an intrinsic behavior. In order to avoid any influence of demagnetization effect caused by sample geometry, sphere-like sample was selected and soaked in the oil together with Pb. No fragmentation was found after the measurements with in situ pressure, indicating that the demagnetization effect can be equally neglectable under various pressures. With increasing magnetic field, the magnetization increases but does not saturate at 5T, reflecting the magnetizing process of the specific non-linear spin structure in HoCuSi. However, a weak but noticeable metamagnetic transition induced by magnetic field can be identified. The critical magnetic field $H_C$ of the metamagnetic transition at different pressures can be quantitatively determined by the peak position of dM/dH vs. H curves (inset of Fig. 3a). The $H_C$ shows a monotonic decrease from 0.35T at 0 kbar to 0.2T at 9.0 kbar (Table 1). This result indicates that the AFM coupling tends to be weak with increasing pressure. A smaller magnetic field can destroy the AFM coupling at a higher pressure, inducing the metamagnetic transition. Moreover, the magnetization exhibits a much more rapid tendency towards saturation as a higher pressure is applied. These results further demonstrate that the FM coupling is strongly favored by pressure. The regulation of magnetization process by pressure leads to different magnetization at a given magnetic field. As a representative display, Fig. 3b shows the pressure dependence of magnetization at 1T, 2T and 5T collected at 5 K. It can be seen that the all 1T, 2T and 5T magnetization show rapid growth when the applied pressure is lower than 6.6 kbar, while the growth ratio gradually declines with increasing magnetic field, which is ~46%, ~28%, and ~11% for 1T, 2T, and 5T magnetization,

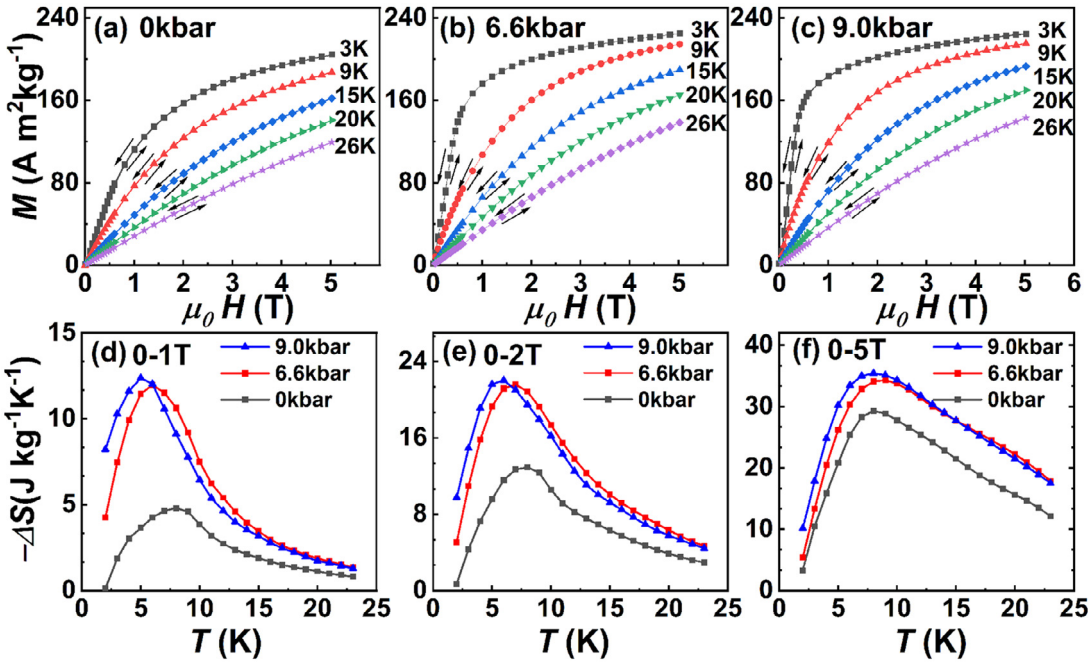


**Fig. 4.** Magnetization isotherms of HoCuSi measured on increasing and decreasing fields under (a) ambient pressure, (b) 6.6 kbar, (c) 9.0 kbar, where the arrows indicate the ramping direction of magnetic field. Entropy change ΔS under different pressures at (d)0–1T, (e)0–2T, and (f)0–5T magnetic field change. (For interpretation of the references to colour in this figure legend, the reader is referred to the web version of this article.)

respectively (Fig. 3b). Further increasing pressure to 9.0 kbar cannot make a notable growth of magnetization particularly for the cases of 2T and 5T. This is a result of the regulation process of pressure on the evolution of the specific non-linear spin structure with magnetic field in HoCuSi, where the change of CFE caused by pressure plays an important role [19,25]. Specifically, at ambient pressure, the 5T magnetization (200.3 $Am^{-2}kg^{-1}$, equivalent to 9.53 $\mu_B/Ho^{3+}$) is still smaller than the magnetic moment of free $Ho^{3+}$ ions (~10.60 $\mu_B/Ho^{3+}$), but the pressure equal to or larger than 6.6 kbar can make the 5T magnetization approach to that of free $Ho^{3+}$ ions. These results illustrate that the actions of pressure and magnetic field are the same, both favoring the FM coupling. Such a modulation process of spin structure by pressure is distinct from the mechanism previously reported, where the pressure may alter the nature of the magnetostructural/magnetoelastic transition and cause hysteresis loss [8,10]. Moreover, MCE was seldom enhanced by pressure. For hexagonal MM'X compounds with magnetostructural transition, applied pressure can drive the transition occurring at lower temperature with ΔS almost unchanged initially, [7,14] but the transition becomes less abrupt and the MCE quickly drops as the pressure reaches a critical value $P = 3.7$~6.0kbar. In present HoCuSi, any state of spin structure driven by pressure is reversible against magnetic field, noting that the M–H curves show completely reversibility at any temperature and pressure (Fig. 3a, Fig. 4a,b,c). Moreover, the significant increasements of magnetization by pressure, particularly under magnetic field lower than 2T (Fig. 3b), predict large enhancements of the reversible MCE and the refrigeration capacity (RC).

To calculate entropy change ΔS, isothermal M–H curves were measured under different pressures around transition temperature for HoCuSi (Fig. 4a,b,c). The application of pressure enhances the magnetization, the same as the M–H curves at 5 K shown in Fig. 3a. The ΔS was calculated using Maxwell relation $\Delta S = \int_0^H (\frac{\partial M}{\partial T})_{P,H} dH$ [1,26]. Fig. 4d,e,f comparably show the temperature dependent ΔS at 0–1T, 0–2T, 0–5T magnetic field change under different pressures, respectively. The ΔS peaks around 8 K. Under ambient pressure, the maximum of -ΔS is about 4.8, 12.9, 29.3 $Jkg^{-1}K^{-1}$ at 0–1T, 0–2T, 0–5T, respectively. These values are somewhat smaller compared to our previously reported [15], possibly due to the difference from sample to sample. Note that excess amount of Ho was added considering its volatilization during preparation. When a 6.6 kbar pressure is applied, the -ΔS increases to 12.0, 21.6, 34.3 $Jkg^{-1}K^{-1}$ at 0–1T, 0–2T, 0–5T, and the enhanced ratio is 150%, 67%, 17%, respectively. Further increasing pressure to 9.0 kbar only slightly enhances the -ΔS, consistent with the behavior of 1T, 2T and 5T magnetization with pressure (Fig. 3b). According to Eq. (1), under low magnetic fields, crystal field interaction dominated by pressure plays a more significant role in regulating the spin structure and increasing magnetic moment, compared to the magnetic field-induced Zeeman interaction and spin-spin coupling. When the magnetic field increases 5T, the Zeeman interaction increases significantly. In this case, the effect of pressure on the crystal field interaction and the spin-spin interaction will become relatively limited. As a result, the pressure-enhanced ratio of magnetization and MCE decline with increasing magnetic field. Additionally, refrigeration capacity $RC = \int_{T_1}^{T_2} |\Delta S| dT$ is another useful parameter to evaluate refrigerant, where $T_1$ and $T_2$ refer to the temperatures corresponding to the full width at half maximum (FWHM) in the ΔS curves. For HoCuSi, RC is equal to effective $RC_{eff}$ because no hysteresis occurs at any temperature and pressure [27]. The calculated $RC_{eff}$ along with the ΔS at various magnetic fields and pressures are also summarized in Table 2. The zero pressure RC is about 36, 109, 389 $Jkg^{-1}$ at 0–1T, 0–2T, 0–5T, which remarkably increases to 84, 189, 533 $Jkg^{-1}$ with enhanced ratio 134%, 73%, 37%, respectively, when a 6.6kbar pressure was applied. Further increasing pressure to 9.0kbar only slightly enhances the RC. These results are consistent with the behavior of 1T, 2T and 5T magnetization and the ΔS with pressure (Table 2).

In summary, large enhancement of reversible MCE driven by hydrostatic pressure has been demonstrated in HoCuSi compound. When a 6.6 kbar pressure is applied, the reversible -ΔS and $RC_{eff}$ around 8 K increase by 150% and 134%(0–1T), 67% and 73%(0–2T), respectively, under the magnetic field available by permanent

**Table 2**
The entropy change -ΔS, refrigeration capacity $RC_{eff}$ and the correspondingly enhanced ratio of -ΔS and $RC_{eff}$ for HoCuSi under different magnetic fields and pressures.

| | 0–1T | | | | 0–2T | | | | 0–5T | | | |
|---|---|---|---|---|---|---|---|---|---|---|---|---|
| P.kbar | -ΔS.(J $kg^{-1}K^{-1}$) | Enh. -ΔS | $RC_{eff}$.(J/kg) | Enh. $RC_{eff}$ | -ΔS.(J $kg^{-1}K^{-1}$) | Enh. -ΔS | $RC_{eff}$.(J/kg) | Enh. $RC_{eff}$ | -ΔS.(J $kg^{-1}K^{-1}$) | Enh. -ΔS | $RC_{eff}$.(J/kg) | Enh. $RC_{eff}$ |
| 0 | 4.8 | – | 36 | – | 12.9 | – | 109 | – | 29.3 | – | 389 | – |
| 6.6 | 12.0 | 150% | 84 | 134% | 21.6 | 67% | 189 | 73% | 34.3 | 17% | 533 | 37% |
| 9.0 | 12.4 | 158% | 90 | 152% | 22.0 | 71% | 190 | 75% | 35.4 | 21% | 555 | 43% |

magnet. The underlying origin is revealed. Applied pressure regulates the non-collinear spin structure and magnetization process through the competitions of crystal field interactions and spin-spin coupling. The driven state of spin structure by pressure shows completely reversibility against magnetic field, hence the significantly enhanced MCE still keeps reversible. The mechanism is distinct from the pressure driven magnetostructural/magnetoelastic transition previously reported. The large enhancement of reversible ΔS and $RC_{eff}$ is beneficial for developing hybrid field driven refrigeration applications at low temperature regions.

## Declaration of Competing Interest

The authors declare that they have no known competing financial interests or personal relationships that could have appeared to influence the work reported in this paper.

## Acknowledgments

This work was supported by the National Key Research and Development Program of China (Grant Nos. 2017YFB0702702, 2019YFA0704904, 2018YFA0305704, 2017YFA0206300, 2017YFA0303601, and 2016YFB0700903), the National Natural Science Foundation of China (Grant Nos. U1832219, 51531008, 51771223, 51590880, 51971240, 11674378, 11934016, 11921004), and the Key Program and Strategic Priority Research Program (B) of the Chinese Academy of Sciences.

## Supplementary materials

Supplementary material associated with this article can be found, in the online version, at doi:10.1016/j.scriptamat.2020.04.019.

## References

[1] K.A. Gschneidner Jr, V.K. Pecharsky, A.O. Tsokol, Rep. Prog. Phys. 68 (6) (2005) 1479–1539.
[2] A. Smith, C.R.H. Bahl, R. Bjørk, K. Engelbrecht, K.K. Nielsen, N. Pryds, Adv. Energy Mater. 2 (11) (2012) 1288–1318.
[3] A.G. Gamzatov, A.M. Aliev, A. Ghotbi Varzaneh, P. Kameli, I. Abdolhosseini Sarsari, S.C. Yu, Appl. Phys. Lett. 113 (17) (2018) 172406.
[4] D.M. Liu, M. Yue, J.X. Zhang, T.M. McQueen, J.W. Lynn, X.L. Wang, Y. Chen, J.Y. Li, R.J. Cava, X.B. Liu, Z. Altounian, Q.Z. Huang, Phys. Rev. B 79 (1) (2009) 014435.
[5] Y.X. Wang, H. Zhang, E.K. Liu, X.C. Zhong, K. Tao, M.L. Wu, C.F. Xing, Y.N. Xiao, J. Liu, Y. Long, Adv. Electron. Mater. 4 (5) (2018) 1700636.
[6] B. Li, W.J. Ren, Q. Zhang, X.K. Lv, X.G. Liu, H. Meng, J. Li, D. Li, Z.D. Zhang, Appl. Phys. Lett. 95 (17) (2009) 172506.
[7] L. Caron, N.T. Trung, E. Brück, Phys. Rev. B. 84 (2) (2011) 020414.
[8] J.Z. Hao, F.X. Hu, J.T. Wang, F.R. Shen, Z.B. Yu, H.B. Zhou, H. Wu, Q.Z. Huang, K.M. Qiao, J. Wang, J. He, L.H. He, J.R. Sun, B.G. Shen, Chem. Mater. 32 (5) (2020) 1807–1818.
[9] L. Manosa, A. Planes, Adv. Mater. 29 (11) (2017) 1603607.
[10] T. Samanta, D.L. Lepkowski, A.U. Saleheen, A. Shankar, J. Prestigiacomo, I. Dubenko, A. Quetz, I.W.H. Oswald, G.T. McCandless, J.Y. Chan, P.W. Adams, D.P. Young, N. Ali, S. Stadler, Phys. Rev. B. 91 (2) (2015) 020401(R).
[11] K.M. Qiao, F.X. Hu, Y. Liu, J. Li, H. Kuang, H.R. Zhang, W.H. Liang, J. Wang, J.R. Sun, B.G. Shen, Nano Energy 59 (2019) 285–294.
[12] Y.Y. Gong, D.H. Wang, Q.Q. Cao, E.K. Liu, J. Liu, Y.W. Du, Adv. Mater. 27 (5) (2015) 801–805.
[13] J. Liu, T. Gottschall, K.P. Skokov, J.D. Moore, O. Gutfleisch, Nat. Mater. 11 (7) (2012) 620–626.
[14] R.R. Wu, L.F. Bao, F.X. Hu, H. Wu, Q.Z. Huang, J. Wang, X.L. Dong, G.N. Li, J.R. Sun, F.R. Shen, T.Y. Zhao, X.Q. Zheng, L.C. Wang, Y. Liu, W.L. Zuo, Y.Y. Zhao, M. Zhang, X.C. Wang, C.Q. Jin, G.H. Rao, X.F. Han, B.G. Shen, Sci. Rep. 5 (2015) 18027.
[15] J. Chen, B.G. Shen, Q.Y. Dong, F.X. Hu, J.R. Sun, Appl. Phys. Lett. 96 (15) (2010) 152501.
[16] V. Franco, J.S. Blázquez, J.J. Ipus, J.Y. Law, L.M. Moreno-Ramírez, A. Conde, Prog. Mater Sci. 93 (2018) 112–232.
[17] H. Wada, S. Tomekawa, M. Shiga, Cryogenics (Guildf) 39 (11) (1999) 915–919.
[18] L.W. Li, M. Yan, J. Alloys Compd. 823 (2020) 153810.
[19] A. Oleś, R. Duraj, M. Kolenda, B. Penc, A. Szytuła, J. Alloys Compd. 363 (1–2) (2004) 63–67.
[20] S. Gupta, K.G. Suresh, A. Das, A.K. Nigam, A. Hoser, APL Mater. 3 (6) (2015) 066102.
[21] P. Javorský, J. Prchal, D. Adroja, Solid State Commun. 146 (1–2) (2008) 21–24.
[22] M.T. Hutchings, Solid State Phys. 16 (1964) 227–273.
[23] M.W. Dirken, R.C. Thiel, K.H.J. Buschow, J. Less-Common Met. 147 (1) (1989) 97–104.
[24] M.B. Gomes, N.A. de Oliveira, J. Magn. Magn. Mater. 320 (14) (2008) e153–e155.
[25] R.J. Radwanski, R. Michalski, Z. Ropka, A. Blaut, Phys. B (Amsterdam, Neth.) 319 (1–4) (2002) 78–89.
[26] P.J.v. Ranke, N.A. de Oliveira, C. Mello, A.M.G. Carvalho, S. Gama, Phys. Rev. B 71 (5) (2005) 054410.
[27] V. Provenzano, A.J. Shapiro, R.D. Shull, Nature 429 (6994) (2004) 853–857.